Temporal variability of visibility and its parameterizations in Ningbo, China

Jingjing Zhang, Lei Tong, Chenghui Peng, Huiling Zhang, Zhongwen Huang, Jun He, Hang Xiao

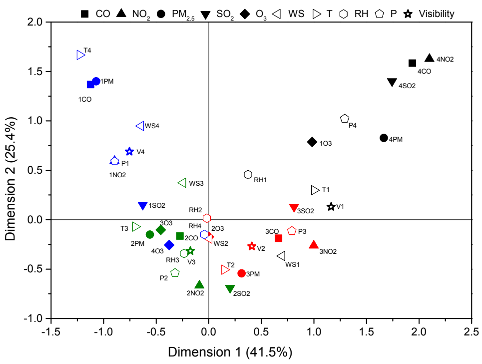

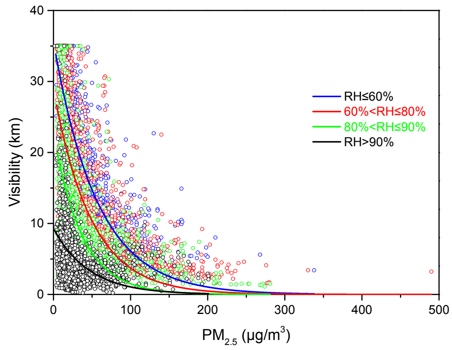

Temporal variability of visibility and its parameterizations in Ningbo, China

Jingjing Zhang[a,b,c,1], Lei Tong[a,b,1], Chenghui Peng[b,c], Huiling Zhang[a,c], Zhongwen Huang[a,c,d], Jun He[e], Hang Xiao[a,b,*]

[a] *Center for Excellence in Regional Atmospheric Environment, Institute of Urban Environment, Chinese Academy of Sciences, Xiamen 361021, China*

[b] *Key Lab of Urban Environment and Health, Institute of Urban Environment, Chinese Academy of Sciences, Xiamen 361021, China*

[c] *University of Chinese Academy of Sciences, Beijing 100049, China*

[d] *School of Chemistry and Environmental Engineering, Hanshan Normal University, Chaozhou, 521041, China*

[e] *International Doctoral Innovation Centre, Department of Chemical and Environmental Engineering, University of Nottingham Ningbo China, Ningbo, China*

---

*Corresponding author. Institute of Urban Environment, Chinese Academy of Sciences, Xiamen, China.

E-*mail address*: hxiao@iue.ac.cn

[1] The authors contributed equally to this article.

Temporal variability of visibility and its parameterizations in Ningbo, China

Jingjing Zhang[a,b,c,1], Lei Tong[a,b,1], Chenghui Peng[b,c], Huiling Zhang[a,c], Zhongwen Huang[a,c,d], Jun He[e], Hang Xiao[a,b,*]

[a] *Center for Excellence in Regional Atmospheric Environment, Institute of Urban Environment, Chinese Academy of Sciences, Xiamen 361021, China*
[b] *Key Lab of Urban Environment and Health, Institute of Urban Environment, Chinese Academy of Sciences, Xiamen 361021, China*
[c] *University of Chinese Academy of Sciences, Beijing 100049, China*
[d] *School of Chemistry and Environmental Engineering, Hanshan Normal University, Chaozhou, 521041, China*
[e] *International Doctoral Innovation Centre, Department of Chemical and Environmental Engineering, University of Nottingham Ningbo China, Ningbo, China*

Abstract: Simultaneous and continuous measurements of visibility, meteorological parameters and the concentrations of six atmospheric pollutants (PM_{10}, $PM_{2.5}$, SO_2, NO_2, CO and O_3) were determined at a suburban site of Ningbo, Eastern China from June 1, 2013 to May 31, 2015. The characteristics of visibility and relationships with air pollutants and meteorological factors were investigated using multiple statistical methods. Daily visibility ranged from 0.6 km to 34.1 km, with a mean value of 11.8 km. During the 2-years' experiment, 43.4% of daily visibility was found to be less than 10.0 km and only 9.2% was greater than 20.0 km. Visibility was lower in winter with a frequency of 53.4% in the range of 0.0–5.0 km. Annual visibility had an obvious diurnal variation, with the lowest and highest visibility being 7.5 km at approximately 06:00 local time and 15.6 km at approximately 14:00 local time, respectively. Multiple correspondence analysis (MCA) indicates that visibility shows significant correlations with concentrations of pollutants and meteorological conditions. Based on the analyses, visibility is found to be the exponential function of $PM_{2.5}$ concentration within a certain range of relative humidity. Thus, non-linear models combining multiple linear regressions with exponential regression were subsequently developed using the data collected from June 2014 to May 2015, and the data from June 2013 to May 2014 was used to evaluate the performance of the model. It was demonstrated that the derived models can quantitatively describe the relationships between visibility, air quality

*Corresponding author. Institute of Urban Environment, Chinese Academy of Sciences, Xiamen, China.
E-*mail address*: hxiao@iue.ac.cn
[1] The authors contributed equally to this article.

and meteorological parameters in Ningbo.

Keywords: Visibility; Multiple correspondence analysis (MCA); Multiple non-linear regression

Introduction

Horizontal visibility is defined as the greatest distance at which a black object can be visually identified with unaided eyesight against a light sky (Wark et al. 1998; Watson 2002). In the absence of unusual weather, the reduction of visibility is an important indicator of deteriorating ambient air quality which has become a serious environmental issue of public concern in populated cities and has been reported to have adverse effects on human health, crop growth and traffic safety (Che et al. 2006). It has been widely confirmed that the impairment of visibility is mainly due to the scattering and absorption of visible light by suspended particles (Chan et al. 1999; Horvath. 1995).

Atmospheric particulate matter (PM) is associated with both anthropogenic and natural emissions that consist of minuscule particles of solid or liquid matter, with diameters ranging from 0.01 μm to 100 μm. Atmospheric particles can affect the climate by both direct and indirect radiative forcing (Charlson et al. 1992; Xu et al. 2002), especially fine aerosols with aerodynamic diameters of 2.5 μm or less ($PM_{2.5}$). The smaller a particle, the longer it will remain suspended in atmosphere and impact the environment over greater distances. In addition, many studies have shown that fine particles, which include sulfates, nitrates, organic and elemental carbon, could effectively scatter or absorb visible light and thus reduce visibility (Zhang et al. 2012; Kim et al. 2006; Tan et al. 2009a, 2009b). All these airborne particles, together with other gaseous pollutants such as sulfur dioxide (SO_2) and nitrogen oxides (NO_x) could contribute to the increase of haze and lead to a low visual range (≤10 kilometers). Specifically, the heterogeneous aqueous transformation from SO_2 and NO_x is enhanced during haze episodes, which probably leads to the remarkable secondary formation of sulfate and nitrate in fine particles, further impairing visibility (Wang et al. 2006). In addition to air pollutants, many meteorological parameters such as relative humidity (RH), wind speed (WS) and direction (WD), temperature, pressure and precipitation can also contribute to light extinction and degrade air quality (Zhao et al. 2011; Yang et al. 2007). In haze events, the rapid increase of PM concentrations, high RH, and low WS, can simultaneously adversely impact atmospheric visibility (Tsai, 2005; Zhang et al. 2010; Deng et al. 2011). As RH increases, hygroscopic particles progressively absorb more moisture, which will increase the scattering cross section of aerosols and proportionately reduce visibility. Therefore, RH could directly affect the particles that contribute to visibility reduction. While other meteorological variables such as WS, temperature, and pressure have indirect effects on visibility, they may also affect the concentration of atmospheric particles due to the thermal and mechanical turbulence (Du et al. 2013). The accumulation and transport of particles are closely related to the synoptic systems and atmospheric circulations. Tsai (2005) identified that conditions for reducing visibility included high atmospheric pressure, low WS, and low mixing layer height. Deng et al. (2011) have also highlighted the significant impact of synoptic systems on air pollution and visibility in Nanjing.

The forecasting and early warning of visibility, which mainly based on the relationships between air pollution and light extinction, is not only very important for environment and public health, but also for traffic control and even military. A number of models were previously developed to describe the correlations between visibility and air pollution, and much continuous efforts have been made to improve the models based on the monitoring results of visibility meter. Wen and Yeh (2010) established multiple linear regression equations linking visibility and atmospheric air conditions for data collected in Taiwan. Both Lin et al. (2012) and Tsai (2005) developed empirical regression models for visibility, with a logarithm of coarse particle concentration used in the regression analyses. Additionally, several studies have suggested that visibility is a linear response to the exponential function of $PM_{2.5}$ concentrations under a certain RH range (Cao et al. 2012; Yu et al. 2016; Shen et al. 2016). All these studies suggested that the impacts of air quality and other variables on visibility are more complicated than linearity and need to be studied further.

In recent decades, four major regions in China (i.e. Beijing-Tianjin-Hebei region, the Yangtze River Delta (YRD) region, the Sichuan Basin, and the Pearl River Delta (PRD) region), have experienced a severe loss of visibility (Zhang et al. 2012). Ningbo is one of the most highly urbanized and industrialized cities in the YRD region and had a population of 7.87 million people and a vehicle fleet of 1.98 million by the end of September 2016. The city is located in the south of Hangzhou Bay and to the west of the East China Sea with an area of 9816 km^2. With a rapid urbanization and an increase in motor vehicle numbers, Ningbo energy consumption has increased substantially and haze events have been frequently observed in recent years (He et al. 2016; Cheng et al. 2014; Hua et al. 2015). Local visibility might be significantly influenced by the increasing frequency of haze episodes. However, there have been few studies focusing on the characteristics of visibility, and their relationships with air pollutants in Ningbo.

In this study, visibility was monitored from June 2013 to May 2015, with potential relationships between visibility and a range of air pollutants (i.e. SO_2, NO_2, CO, O_3, PM_{10}, and $PM_{2.5}$) and meteorological variables (i.e. RH, WS, temperature, and atmospheric pressure) being investigated. The objectives of this study were (1) to characterize the temporal variations of visibility in the suburb of Ningbo; (2) to identify the relationships between classified visibility and other parameters using multiple correspondence analysis (MCA); (3) to develop a regression model suitable for the prediction of visibility in Ningbo based on air pollutant data and meteorological parameters.

1 Material and Methods

1.1 Study Area and Data Source

Ningbo (28°51′–30°33′ N, 120°55′–122°16′ E) is a coastal city of the Zhejiang Province in Eastern China. The climate conditions of Ningbo are governed by the sub-tropical monsoon, with prevailing northwest and southeast winds in winter and summer, respectively. The annual mean air temperature and precipitation are 16.4℃ and 1,480 mm, respectively. Annual mean air temperature reaches its maximum (28.0℃) in July and minimum (4.7℃) in January. During the whole year, approximately 60% of the annual mean precipitation occurs from May to September. The annual mean WS is 2–3 m/s in urban areas and > 5 m/s in coastal areas.

Air pollutant concentrations and meteorological data collected from June 1, 2013 to May 31, 2015 at the Dongqian Lake (DQL) Monitoring Station (29°45′N, 121°37′E) were used in this study. The monitoring station is 12 km away from the city center of Ningbo and 1.3 km from the biggest freshwater lake (Dongqian Lake, 22 km^2 in area) in the Zhejiang Province. There are several hills nearby to the west and east. Many small villages are distributed at the mountain foot less than 2 km to DQL site. There is a provincial road close to this site with small factories involved in mechanical processing built alongside. In recent years, the tourism resources around DQL have been greatly developed, with increasing numbers of urban residents visiting the area for recreational purposes.

The DQL station is a part of the national air quality monitoring network of China, which is under the supervision of the national Ministry of Environmental Protection (MEP). Visibility is measured by trained operators using easily identifiable structures and objects, such as tall buildings, towers, and mountain ridges, at predetermined distances. The routine monitoring of air quality with six conventional indices (i.e. SO_2, CO, NO_2, O_3, PM_{10}, $PM_{2.5}$) at DQL station began in 2012 when the latest ambient air quality standards of China (GB 3095-2012) were established. Commercial instruments from Thermo-Fisher Scientific Inc. (USA) are used to measure gaseous pollutants, such as O_3 (Model 49i), NO_2 (Model 42i), CO (Model 48i) and SO_2 (Model 43i). $PM_{2.5}$ and PM_{10} are measured using a tapered-element oscillating microbalance sampler (R&P TEOM, 1400). The TEOM sampler is calibrated regularly by using filters with measured masses. Zero and span checks are made weekly. Hourly averaged data were used for all analyses in this study and described by local time (UTC+8). Meteorological variables including RH, WS, temperature, and atmospheric pressure are measured by automatic weather station (WS500-UMB, Lufft, Germany) at DQL site. The fire count map was retrieved from FIRMS Web Fire Mapper (NASA, https://earthdata.nasa.gov/).

The Air Quality Index (AQI) has been developed to provide daily air quality information to the public in China (Zheng et al., 2014). On February 29, 2012, the Ministry of Environmental Protection (MEP) of the People's Republic of China (PRC) approved the technical regulation on ambient air quality index (GB 3095-2012), which released $PM_{2.5}$ values and calculated the AQI instead of the Air pollution Index (API). A sub-index is calculated for each pollutant from a segmented linear function that transforms ambient concentrations onto a scale from 0 to 500. AQI is calculated as the sub-index maximum (China's Environmental Protection Standards, HJ 633-2012). Daily AQI is defined as:

$$\mathrm{AQI} = \max\left(\mathrm{AQI}_{PM_{10}}, \mathrm{AQI}_{PM_{2.5}}, \mathrm{AQI}_{SO_2}, \mathrm{AQI}_{NO_2}, \mathrm{AQI}_{CO}, \mathrm{AQI}_{O_3}\right) \quad (1)$$

where $\mathrm{AQI}_{PM_{10}}$, $\mathrm{AQI}_{PM_{2.5}}$, AQI_{SO_2}, AQI_{NO_2}, AQI_{CO} and AQI_{O_3} are the partial index of air pollutants PM_{10}, $PM_{2.5}$, SO_2, NO_2, CO and O_3, respectively.

$$\mathrm{AQI}_p = [(\mathrm{AQI}_{ph} - \mathrm{AQI}_{pl}) / (C_{high} - C_{low})] \times (C_p - C_{low}) + \mathrm{AQI}_{pl} \quad (2)$$

where AQI_p is the partial index of air pollutant p, C_p is the daily average concentration of air pollutant p, C_{high} and C_{low} are the threshold concentrations of p at air quality grade, respectively. Corresponding to C_{high} and C_{low}, AQI_{ph} and AQI_{pl} are the threshold partial indexes of air pollutant p at air quality grade, respectively.

1.2 Data Analysis

Multiple correspondence analysis (MCA) is a data analysis technique for categorical data, used to detect and represent the underlying relationships in a data set. It is complementary to analytical models as the reduction and display of contingency tables produces graphics, which could depict the structural relationships among categories within variables (Hair et al. 1995; Hill et al. 2007). The purpose of MCA, also known as homogeneity analysis, is to find quantifications that are optimal in the sense that the separation of categories is maximised. This implies that objects in the same category are plotted close to each other and objects in different categories are plotted as far apart as possible. The analysis is most successful when the variables are homogeneous; that is, when they partition objects into clusters with the same or similar categories. This statistical method has been widely used in sociology, economic statistics, medical science, but is still limited in environmental science (Van Stan et al. 2016; Sourial et al. 2010).

2 Results and Discussion

2.1 Overall Results of the Study Area

The overall statistical analysis of daily visibility, air pollutants, and meteorological variables during the two years of observations at DQL station are summarized in **Table S1**. Day-to-day variations of visibility, $PM_{2.5}$ and PM_{10} are shown in **Fig. S1**. From June 1, 2013 to May 31, 2015, the daily average visibility ranged from 0.6–34.1 km, with a mean value of 11.8 km, which was just over the defined threshold for haze (i.e. visibility < 10.0 km), indicating poor air quality over the study region. The mean $PM_{2.5}$, PM_{10}, SO_2, NO_2, CO and O_3 concentrations were 42.6 μg/m^3, 64.6 μg/m^3, 15.0 μg/m^3, 28.9 μg/m^3, 0.9 mg/m^3 and 70.2 μg/m^3, respectively. The average value of AQI, RH, temperature, WS and surface pressure were 65.6, 73.2%, 17.8℃, 1.7 m/s and 1013.0 hPa, respectively.

Visibility impairment mainly resulted from airborne particulate matter, particularly from fine particles with aerodynamic diameters less than 2.5 μm (Deng et al. 2014; Sabetghadam and Ahmadi-Givi 2014). According to air quality daily report from MEP, $PM_{2.5}$ in the atmosphere was the primary pollutant of concern in Ningbo during the two years (http://www.zhb.gov.cn). Therefore, the daily variations of PM_{10} and $PM_{2.5}$ were required for analysis during the study period in DQL station. Fig. S1 shows that the concentrations of $PM_{2.5}$ and PM_{10} were generally higher in winter and lower in summer, and the proportion of $PM_{2.5}$ in PM_{10} was relatively high. During the two years, almost all daily $PM_{2.5}$ concentrations in winter exceeded the national ambient air quality standard GradeⅡ (75 μg/m^3), revealing severe pollution from fine particles. In December, 2013, extremely high levels of PM_{10} and $PM_{2.5}$ were observed with daily average concentrations of 511 and 389 μg/m^3, respectively. At 22:00 on December 6, the hourly concentrations of PM_{10} and $PM_{2.5}$ reached peak values of 707 and 530 μg/m^3, respectively. Visibility dramatically decreased to 0.6 km during this episode, which was the minimum value measured during the two years. This haze episode was also observed by Xue et al. (2015) in the YRD region.

2.2 Seasonal and Diurnal Variation of Visibility

Fig. 1(a) shows that 43.4% of the daily visibility was less than 10.0 km during the two years and only 9.2% was greater than 20.0 km, indicating bad air quality in DQL area. The maximal frequency (33.4%) of daily visibility was observed in the range of 5.0–10.0 km. Poor visibility

(<5.0 km) often occurred in winter with a frequency of 53.4%. Daily visibilities of spring and summer contributed as much as 41.8% and 38.8% to the visual range of 20.0–35.0 km, respectively.

Generally, the average value of AQI decreased with increasing visibility (**Fig. 1**). The mean value of AQI for the visual range of 0–5.0 km was 111.8 (≥100), which indicates the occurrence of a haze episode under low visibility. The AQI values were 72.3 and 61.4 for the visual range of 5.0–10.0 km and 10.0–15.0 km, respectively. This indicates that the local air was moderately polluted. Good visibility (15.0–35.0 km) occurred simultaneously with the lowest AQI value (<50) i.e. when the air quality was good. These data confirm that the local air quality had an obvious positive correlation with visibility (Tsai et al. 2003).

Fig. 1(b) depicts the diurnal patterns of annual and seasonal mean visibility in Ningbo. Visibility shows an obvious and similar diurnal variation throughout four seasons, with a sharp decrease in early morning, i.e. 06:00-08:00 local time and a peak in afternoon, i.e. 14:00-16:00 local time. From the perspective of the annual average, the lowest and highest visibility was 7.5 km and 15.6 km, respectively. The diurnal patterns during different seasons were desynchronized, which is due to the difference in weather pattern (i.e. day-night length, sunrise and sunset time, monsoon etc.) and the stability of atmospheric boundary layer (ABL) in each season. For example, the trough and peak of visibility in wintertime are nearly two hours later than summertime, which is mainly attributed to a later sunrise time and smaller ABL depth. It can also be seen that visibility in spring and summer was better than autumn and winter, and winter is more likely associated with poor visibility and bad air quality.

2.3 Monthly Variations of Visibility and Environmental Factors

Monthly variations of visibility, air pollutant concentrations and meteorological factors were investigated in this study (**Fig. 2**). The highest average visibility was observed in July, with a value of 16.6 km, and the lowest average visibility was observed in December with a value of 9.1 km. Different trends of monthly variations were observed between visibility and other environmental variables in the study area (**Fig. 2**). It was noteworthy that the visibility greatly decreased in June, when the air pollutant concentrations stayed at low levels. As is well known that visibility is negatively correlated with air humidity (Deng et al., 2011). The relatively high level of RH in June (**Fig. 2**) might account for the lower visibility due to the light scattering and absorption of water vapour.

Fig. 2 shows that the PM_{10} and $PM_{2.5}$ pollution of the study area was severe. The monthly mass concentrations of PM_{10} and $PM_{2.5}$ were in the range of 34.7–139.3 and 23.7–94.9 $\mu g/m^3$, respectively. The concentrations of PM_{10} and $PM_{2.5}$ were higher from November to February, while lower from June to September. The temporal variations of anthropogenic emissions and weather conditions might account for the seasonal cycle of PM. The average ratio of $PM_{2.5}$ to PM_{10} ($PM_{2.5}/PM_{10}$) was 66.6% with a range of 59.3%–72.1%. Remarkably, there was an obvious inverse correlation between visibility and the ratio of $PM_{2.5}/PM_{10}$, especially in June, July and October. The high proportions of $PM_{2.5}$ contained within PM_{10} in poor visibility episodes indicated that fine particles could play an important role in affecting local visibility.

The monthly variations of SO_2, NO_2 and CO were consistent with that of PM, with higher and lower concentrations being observed in winter and summer, respectively. All three gaseous pollutants showed non-significant correlation with visibility. However, a strong correlation between O_3 and visibility was observed during the study period (**Fig. 2**). Two monthly peaks of O_3 were observed in May (100.3 $\mu g/m^3$) and October (71.4 $\mu g/m^3$) along with better visibility, while the lowest O_3 concentration (41.4 $\mu g/m^3$) occurred in December when lower visibility was observed. The winter minimum O_3 level is commonly observed in mid-latitude locations in the Northern Hemisphere (Tu et al. 2007; Semple et al. 2012; kumar et al. 2010), which is mainly due to the relatively weaker photochemical processes. Good visibility is often related to stronger solar radiation, which can significantly promote the photochemical generation of O_3 (Pudasainee et al. 2006). This might account for the good correlation between O_3 levels and visibility during warm seasons in this study.

The variation of RH displayed a summer maximum and winter minimum, with the highest (82.1%) and lowest (62.3%) values occurring in June and December, respectively. Clear positive and negative correlations existed between RH and $PM_{2.5}/PM_{10}$, and between RH and visibility, respectively. With the increase of RH, the generation of secondary aerosols in fine particles was enhanced and the hygroscopic components of aerosols such as sulfate, nitrate and sea salt absorbed more moisture, which would increase the scattering cross section of the aerosols and reduce visibility (Jung et al. 2009).

Obvious monthly variations of surface WS were observed in the study area, with the highest value (2.4 m/s) occurring in July and the lowest value (1.4 m/s) occurring in November (**Fig. 2**). Monthly visibility was positively correlated with WS during most months, especially in summer (June-August) and autumn (September-November). Generally, the increase of WS accelerates the diffusion of dust and pollutants, which leads to an increase of the visual range. Meanwhile, the temperature and pressure also changed obviously in different months. Temperature was highest (29.5°C) in July and lowest (7.0°C) in December, while the barometric pressure was highest (1025.9 hPa) in December and lowest (1005.1 hPa) in July. In general, the variation of visibility was consistent with that of temperature and opposite to that of pressure. The correlations between visibility and temperature and pressure might be accounted for by the following reasons. High air temperature and low pressure usually enhances the dispersal capability of the atmosphere via thermal and mechanical turbulence, which could promote the improvement of air quality and visibility and inversely, low temperature and high pressure indicate more stable weather condition, which would weaken the diffusion of air pollutants.

2.4 Multiple Correspondence Analysis of Visibility

In multiple correspondence analysis, all variables were divided into four categories according to the values from small to large (**Table S2**). In the following discussion, the Arabic 1 to 4 were used to represent the four categories respectively; the category indicator was added as a prefix for air pollution; and as a suffix for meteorological parameter. The correspondence map and loading factors of visibility and other environmental variables based on MCA are shown in **Fig. 3** and **Table S3**, respectively. Most of the variance in our data was accounted for in the analysis with axes 1 and 2 explaining 41.5% and 25.4% variation, respectively. Almost all air pollutants and meteorological factors were classified into four quadrants in the map. The relative distance between variables and the closeness of points on the map with respect to their angle from the origin, and points in the same quadrant can be used to interpret relationships between variables (Higgs et al. 1991; Garson et al. 2012). The origin on the map corresponds to the centroid of each variable. The closer a variable is to the origin, the closer it is to the average profile. As shown in **Fig. 3**, V2 and V3 was near the origin and was the primary visual range during the study period, as described above. During the study period, the frequency of daily visibility appearing in the range of 5.0–15.0 km was higher than those of others (**Fig. 1**). In addition, $4NO_2$, 4CO and $4SO_2$ were located far from the origin in the first quadrant and therefore had the greater variability. This implied that the concentration of air pollutants were inclined to have the greatest effect compared to other factors during the poor visual range (V1 <5 km). Along dimension 2, it was observed that T4, $1PM_{2.5}$, 1CO and WS4 had the most effect, indicating that the lower concentrations of pollutants except for O_3, higher temperature and higher wind speed had a significant influence on good visibility (V4 > 15km).

Fig. 3 illustrates that the first two dimensions accounted for 66.9% of the total variance and the majority of variables were clearly discriminated in both dimensions. Along dimension 1, values of $PM_{2.5}$, SO_2, CO, NO_2 and P increased positively with the direction of dimension 1. Conversely, T, V and WS decreased in dimension 1. However, only WS along dimension 2 changed regularly, which increased in a positive direction. Generally, dimension 1 could account for most air pollutants, P, T, V and WS; and dimension 2 only explained WS additionally. However, the two dimensions in our study could not well represent the variations of O_3 and RH, and the lower loading factors of O_3 and RH in Table S3 also confirmed this.

The variation of O_3 concentrations and RH did not regularly change with dimension 1 or 2, indicating that further dimensions may need to be analysed, i.e. the variation of O_3 has unique characteristics. As previously discussed, visibility was usually positively related with O_3 concentrations. $4O_3$ was closely distributed with V3 rather than V4 in the correspondence map (**Fig. 3**), but the concentration of O_3 did not increase with visibility completely. In fact, except for the lower concentrations of O_3, the points of $2O_3$ to $4O_3$ were all closely placed within the third quadrants of **Fig. 3**, which were generally associated with a relatively higher temperature and lower WS. The relatively high WS (WS4 & WS3) in the second quadrant was unfavourable to the accumulation of O_3. These data also indicated that the production of O_3 was not only affected by visibility, other pollutants and meteorological parameters, but also factors including solar radiation, which was not included in this study (Tong et al., 2017). In addition, the effects of RH on visibility could not be ignored. The visibility was always below 15 km (V1 ~ V3) when RH was higher than 80% (i.e. RH3 & RH4), which indicated that visibility remained at low values even with low air pollution concentrations.

2.5 Relationship Between Visibility and Other Factors

To gain a deeper insight into how relevant factors affect visibility, Pearson correlations were performed between daily visibility, air pollutants and meteorological variables (**Table S4**). Visibility had significantly negative correlations with $PM_{2.5}$ (r = –0.50), CO (r = –0.51), and NO_2 (r = –0.47). The moderate relationship between visibility and $PM_{2.5}$ was expected, given the scattering effect of aerosols, especially fine aerosols with aerodynamic diameters of 2.5μm or less (Charlson et al. 1992; Xu et al. 2002). Visibility had no direct relationship with CO, but the correlation coefficient between both variables was a little higher than that between visibility and $PM_{2.5}$. This may be because CO is generated by intensive biomass burning together with incomplete combustion from vehicle engines, during which large quantities of particles would be generated. Fine particles formed simultaneously with CO could lead to visibility reduction by scattering and absorbing light radiation (Xue et al. 2015), which might account for the negative correlation between visibility and CO. For NO_2, there was a weak direct influence on visibility. However, secondary pollutants such as nitrate, which is produced by photochemical conversions from NO_2 might play an important role in visibility reduction (Sabetghadam and Ahmadi-Givi 2014). Nitrate is the main water-soluble constituent in $PM_{2.5}$ and is an important factor in the increase of $PM_{2.5}$ concentrations. A strong positive correlation between NO_2 and $PM_{2.5}$ (r= 0.70, Table S4) was observed in this study, which might explain why NO_2 was significantly correlated with visibility in the DQL area.

In analyses examining effects of meteorological factors, visibility showed a significant positive correlation (r= 0.39) with WS and negative correlation (r= –0.40) with RH, which was in accordance with previous research (Deng et al. 2011; Zhang et al. 2015). High wind speed would promote the dispersion of pollutants and could reduce air pollutant concentrations and increase visibility. Also, hygroscopic aerosols are greatly increased with high RH, which could cause the increase of PM concentration and extinction capability, further reducing visibility. As presented in **Table S4**, visibility showed a rather weak negative and positive correlation with air pressure and temperature, respectively. Air pressure and temperature are both important indicators of weather system at a given location, and they have no direct effect on visibility. The changes of air pressure and temperature could have an impact on the diffusivity of atmosphere, and further affect the concentration of air pollutants. The relatively high correlation between $PM_{2.5}$ and temperature (r= –0.45), and between $PM_{2.5}$ and pressure (r= 0.43) also confirmed this conclusion.

Scatter plots and regression functions of one-year data (**Fig. 4**) were applied in this study in order to examine the deep connections between visibility and the two major factors (i.e. $PM_{2.5}$ and RH). Fig. 4 and obtained equation (3) show the relationships between hourly-averaged visibility and mass concentration of $PM_{2.5}$ under different RH conditions (Yu et al., 2016). RH was classified over four ranges: RH ≤60%, 60 < RH ≤80%, 80 < RH ≤90%, and RH > 90%. The visibility decreased exponentially with increasing $PM_{2.5}$ concentrations in each RH range.

$$\text{Visibility} = f(\text{PM}_{2.5}) = \begin{cases} 35.65 \times \exp(-0.017 \times \text{PM}^{2.5}), & (\text{RH} \leq 60\%),\ r = 0.835 \\ 28.99 \times \exp(-0.020 \times \text{PM}^{2.5}), & (60\% < \text{RH} \leq 80\%),\ r = 0.732 \\ 22.84 \times \exp(-0.027 \times \text{PM}^{2.5}), & (80\% < \text{RH} \leq 90\%),\ r = 0.599 \\ 9.32 \times \exp(-0.021 \times \text{PM}^{2.5}), & (\text{RH} > 90\%),\ r = 0.384 \end{cases} \quad (3)$$

Firstly, with the increase of $PM_{2.5}$ concentration, the visual range decreased exponentially. Initially, the visibility decreased sharply while the $PM_{2.5}$ concentration increased; but when $PM_{2.5}$ concentrations reached a certain level (for example above 100μg/m^3), the change in visibility was not sensitive to $PM_{2.5}$ concentrations any further. Secondly, with the increase of RH, a lower correlation coefficient between $PM_{2.5}$ and visibility was observed. This implied that visibility stayed at a very low level when RH values were very high (>80%), even with low $PM_{2.5}$ concentrations. In this case, a large amount of water vapour could cover particle surfaces, enhancing the scattering ability of aerosol and reduce visibility significantly. Thirdly, the maximum visibility under different RH conditions was decreased with the increase of RH value (**Fig. 4**). Equation (3) suggested that the maximum visibility was just 9.32 km in the case of RH >90%, and this result was consistent with MCA (**Fig. 3**).

Obviously, a single parameter regression as the equation (3) are not suitable for the forecasting of visibility at another location or in another year, which ignores the effects of other environmental variables, such as NO_2, CO, T, WS etc. As presented in **Fig. S2**, in which a separate year's hourly visibility was predicted with equation (3), the regression lines between observed and simulated visibility significantly deviate from the 1:1 diagonal line. A larger deviation existed when RH>90%, indicating a greater contribution of other factors to visibility. Nevertheless, the above equation further confirmed the exponential relationship between visibility and $PM_{2.5}$ under different RH level. This finding should be the basis of a forecasting model of visibility.

2.6 Regression Model Development and Validation

To further develop a brief model for visibility prediction in Ningbo, it was first assumed that the apparent visibility is the final result of a combination of factors influencing air pollution together with meteorological parameters. As shown in Equation (4),

$$Visibility = f(PM_{2.5}) + f(RH, T, NO_2, O_3 \cdots) = f(PM_{2.5}) + \sum_i (a_i \cdot x_i) + \varepsilon \quad (4)$$

where x_i represents any important factor for visibility, a_i is a linear regression coefficient, and ε is the error term.

$$Visibility - f(PM_{2.5}) = \sum_i (a_i \cdot x_i) + \varepsilon \quad (5)$$

or

$$Visibility - \sum_i (a_i \cdot x_i) = f(PM_{2.5}) + \varepsilon \quad (6)$$

The obtained regression parameters in equation (3) were chosen as initial values of modelling fit. Multiple linear regression was conducted between the residue of prediction and other environmental parameters. Datasets with hourly resolution from June 2014 to May 2015 were used to develop the multiple nonlinear regression equations. An independent variable was added into the regression equation by a stepwise procedure based on importance. It demonstrated that for the first two RH categories, i.e. RH≤80%, RH is the common factor in addition to particle concentration for the variation of visibility, then the regression equations for these two levels were eventually combined together. After several circles of regression and iteration, the final modelling results considering main influencing factors besides $PM_{2.5}$ and RH within three RH ranges were listed in **Table 1**. It showed that the main contributors to visibility under different RH are different, and the influence of all variables on visibility was additive. Specifically, the independent variables in the model are $PM_{2.5}$, and RH when RH $\leq$ 80%, while O_3 is the major contributor to the visibility (aside from $PM_{2.5}$ and RH) within RH of 80-90%. The importance of O_3 in the model requires further investigation. Results presented in **Table 1** also suggested temperature can affect visibility when RH > 90%. Likely, temperature affects visibility by influencing condensation of water vapour in the atmosphere.

To further verify the validity of the non-linear models combining exponential and multiple linear regressions, hourly observed visibility data from June 2013 to May 2014 were examined. **Fig. 5** presents the simulated results based on equations in **Table 1** vs. the observed visibility. The newly developed multiple nonlinear model improved the visibility prediction with generally higher R values compared to those based on single parameter regression model (equation 3), especially under high RH (>90%) conditions (**Fig. S2**). Time series of daily observed visibility and daily visibility simulated by nonlinear regression model from June 2013 to May 2014 was plotted in **Fig. 6**. There was a high degree of consistency between model-fitted visibility and observed visibility, indicating that the newly developed model is a suitable and practical model for simulating visibility based on air quality in DQL area.

3 Conclusions

Visibility, atmospheric pollutants and meteorological variables monitored in a suburban area (DQL) of Ningbo from June 1, 2013 to May 31, 2015 were analyzed in this study. The characteristics of visibility and its affecting factors were described in detail using multiple statistical methods. Based on these analyses, the following conclusions can be derived:

The temporal variation of visibility in DQL during the study period demonstrated notable regional characteristics. The seasonal pattern of visibility was characterized by higher levels in spring-summer and lower levels in autumn-winter. Nearly half of all measurements of visibility were lower than 10 km, indicating poor air quality over the study region. Visibility displayed an obvious diurnal variation in each season, with the lowest and highest visibility being 7.5 km at approximately 06:00, and 15.6 km at approximately 14:00, respectively.

The results of multiple correspondence analysis (MCA) indicated that good visibility was always associated with good meteorological conditions and low levels air pollutants, except for O_3. The results of MCA explained 66.9% necessity of the segmented studies of visibility. Based on the correlation analysis, $PM_{2.5}$, WS and relative humidity were found to have significant impacts on visibility in Ningbo. Also, model equations between visibility, PM and RH were derived, with visibility decreasing exponentially with increasing $PM_{2.5}$ concentrations in different RH ranges. Additionally, the non-linear models combining exponential and multiple linear regressions were developed to investigate the underlying relationships between visibility, air quality and meteorological conditions. The main factors which have the largest influences on visibility under different RH ranges are different. Based on comparative evaluation, the model prediction effect is regarded to be relatively good for this suburban area.

This study demonstrated that the correlations between visibility and air pollutants/metrological parameters are relative consistent; and it is possible to predict the visibility based on air quality and weather conditions, although it was based on only two years of data collected from one research station. In order to gain a more accurate understanding of the relationships between visibility and other factors, and to modify the regression equations developed for these Ningbo datasets, analyses on long term and multipoint data are necessary. In addition, the effects of large- and meso-scale phenomena on visibility warrants further study.

Acknowledgments

This work was supported by the National Natural Science Foundation of China (No. 31300435, U1405235), Science and Technology Plan Project of Ningbo City (No. 2015C110001), Natural Science Foundation of Ningbo City (No. 2015A610247), and Knowledge Innovation Program of the Chinese Academy of Sciences (No. IUEQN-2012-03).

References

Cao, J.J., Wang, Q.Y., Chow, J.C., Watson, J.G., Tie, X.X., Shen, Z.X., Wang, P., An, Z.S., 2012. Impacts of aerosol compositions on visibility impairment in Xi'an, China. Atmos. Environ. 59, 559–566.

Chan, Y.C., Simpson, R.W., Mctainsh, G.H., Vowles, P.D., Cohen, D.D., Bailey, G.M., 1999. Source apportionment of visibility degradation problems in Brisbane (Australia) using the multiple linear regression techniques. Atmos. Environ. 33, 3237–3250.

Charlson, R.J.; Schwartz, S.E.; Hales, J.M.; Cess, D.; Coakley, J.A.; Hansen, J.E., 1992. Climate forcing by anthropogenic aerosols. Science 255, 423–430.

Che, H.Z., Zhang, X.Y., Li, Y., Zhou, Z.J., Chen, Z.L., 2006. Relationship between horizontal extinction coefficient and PM_{10} concentration in Xi'an, China, during 1980–2002. Particuology 4, 327–329.

Cheng, Z., Wang, S.X., Fu, X., Watson, J.G., Jiang, J., Fu, Q., Chen, C., Xu, B., Yu, J., Chow, J.C., Hao, J.M., 2014. Impact of biomass burning on haze pollution in the Yangtze River Delta, China; a case study in summer 2011. Atmos. Chem. Phys. 14, 4573–4585.

China Meteorological Administration, 2011. Observation and forecasting levels of haze; QX/T, 113-2010.

Deng, J.J., Wang, T.J., Jiang, Z.Q., Xie, M., Zhang, R.J., Huang, X.X., Zhu, J.L., 2011. Characterization of visibility and its affecting factorsover Nanjing, China. Atmos. Res. 101, 681–691.

Deng, J.J., Xing, Z.Y., Zhuang B.L., Du, K., 2014. Comparative study on long-term visibility trend and its affecting factors on both sides of the Taiwan Strait. Atmos. Res. 143, 266–278.

Du, K., Mu, C., Deng, J.J., Yuan, F., 2013. Study on atmospheric visibility variations and the impacts of meteorological parameters using high temporal resolution data: an application of environmental internet of things in China. Int. J. Sust. Dev. World. 20, 238–247.

Garson, G.D., 2012. Correspondence analysis [Internet]. Statnotes: topics in multivariate analysis. Available athttp://www.statisticalassociates.com/correspondenceanalysis.htm

Hair, J.F., Anderson, R.E., Tatham, R.L., Black, W.C., 1995. Multivariate Data Analysis, fourth ed. Prentice Hall College Division 745 p.

He, T.F., Yang, Z.Y., Liu, T., Shen, Y.P., Fu, X.H., Qian, X.J., Zhang, Y.L., Wang, Y., Xu, Z.W., Zhu, S.K., Mao, C., Xu, G.Z., Tang, J.L., 2016. Ambient air pollution and years of life lost in Ningbo, China. Sci. Rep. 6.

Hill, T., Lewicki, P., 2007. Statistics: Methods and Applications. Statsoft, Tulsa 800 p.

Higgs NT., 1991. Practical and innovative uses of correspondence analysis. Statistician 40, 183–194.

Horvath, H., 1995. Estimation of the average visibility in central Europe. Atmos. Environ. 29, 241–246.

Hua, Y., Chen, Z., Zhang, J.K., Wang, S.X., Jiang, J.K., Chen, D., Cai, S.Y., Fu, X., Fu, Q.Y., Chen, C.H., Xu, B.Y., Yu, J.Q., 2015. Characteristic and source apportionment of $PM_{2.5}$ during a fall heavy haze episode in the Yangtze River Delta of China. Atmos. Environ. 123, 380–391.

Jung, J., Lee, H., Kim, Y.J., Liu, X.G., Zhang, Y.H., Gu, J.W., Fan, S.J., 2009. Aerosol chemistry and the effect of aerosol water content on visibility impairment and radiative forcing in Guangzhou during the 2006 Pearl River Delta campaign. J. Environ. Manage. 90, 3231–3244.

Kim, Y.J., Kim, K.W., Kim, S.D., Lee, B.K., Han, J.S., 2006. Fine particulate matter characteristics and its impact on visibility impairment at two urban sites in Korea: Seoul and Incheon. Atmos. Environ. 40, 593–605.

Kumar, R., Naja, M., Venkataramani, S., Wild, O., 2010. Variations in surface ozone at Nainital: a high-altitude site in the central Himalayas. J. Geophys. Res.-Atmos. 115, 751–763.

Lin, M., Tao, J., Chan, C.Y., Cao, J.J., Zhang, Z.S., Zhu, L.H., Zhang, R.J., 2012. Regression analyses between recent air quality and visibility changes in megacities at four haze regions in China. Aerosol Air Qual. Res. 12, 1049–1061.

Pudasainee, D., Sapkota, B., Shrestha, M.L., Kaga, A., Kondo, A., Inoue, Y., 2006. Ground level ozone concentrations and its association with NO_x and meteorological parameters in Kathmandu valley, Nepal. Atmos. Environ. 40, 8081–8087.

Semple, D., Song, F., Gao, Y., 2012. Seasonal characteristics of ambient nitrogenoxides and ground-level ozone in metropolitan northeastern New Jersey. Atmos. Pollut. Res. 3, 247–257.

Sabetghadam, S., Ahmadi-Givi, F., 2014. Relationship of extinction coefficient, air pollution, and meteorological parameters in an urban area during 2007-2009. Environ. Sci. Pollut. Res. 21, 538–547.

Shen, Z.X., Cao, J.J., Zhang, L.M., Qian, Z., Huang, R.J., Liu, S.X., Zhao, Z.Z., Zhu, C.S., Lei, Y.L., Xu, H.M., Zheng, C.L., 2016. Retrieving historical ambient $PM_{2.5}$ concentrations using existing visibility measurements in Xi'an, Northwest China. Atmos. Environ. 126, 15–20.

Sourial, N., Wolfson, C., Zhu, B., Quail, J., Fletcher, J., Bergman, H., 2010. Correspondence analysis is a useful tool to uncover the relationship among categorical variables. J. Clin. Epi. 63, 638–646.

Tan, J.H., Duan, J.C., Chen, D.H., Wang, X.H., Guo, S.J., Bi, X.H., Sheng, G.Y., He, K.B., Fu, J.M., 2009a. Chemical characteristics of haze during summer and winter in Guangzhou. Atmos. Res. 94, 238–245.

Tan, J.H., Duan, J.C., He, K.B., Ma, Y.L., Duan, F.K., Chen, Y., Fu, J.M., 2009b. Chemical characteristics of $PM_{2.5}$ during a typical haze episode in Guangzhou. J. Environ. Sci. 21, 774–781.

Tong, L., Zhang, H.L., Yu, J., He, M.M., Xu, N.B., Zhang, J.J., Qian, F.Z, Feng, J.Y., Xiao, H., 2017. Characteristics of surface ozone and nitrogen oxides at urban, suburban and rural sites in Ningbo, China. Atmos. Res. 187, 57–68.

Tsai, Y.I., 2005. Atmospheric visibility trends in an urban area in Taiwan 1961–2003. Atmos. Environ. 39, 5555–5567.

Tsai, Y.I., Lin, Y.H., Lee, S.Z., 2003. Visibility variation with air qualities in the metropolitan area in southern Taiwan. Water Air Soil Pollut. 144, 19–40.

Tu, J., Xia, Z.G., Wang, H., Li,W., 2007. Temporal variations in surface ozone and its precursors and meteorological effects at an urban site in China. Atmos. Res. 85, 310–337.

Van Stan, J.T., Gay, T.E., Lewis, E.S., 2016. Use of multiple correspondence analysis (MCA) to identify interactive meteorological conditions affecting relative throughfall. J. Hydro. 533, 452–460.

Wang, Y., Zhuang, G.S., Sun, Y.L., An, Z.S., 2006. The variation of characteristics and formation mechanisms of aerosols in dust, haze, and clear days in Beijing. Atmos. Environ. 40, 6579–6591.

Wark, K., Warner, C.F., Davis, W.T., 1998. Air pollution–its origin and control, 3rd edition, Addison–Wesley, MA, United States, 573 p.

Watson, J.G., 2002. Critical review discussion-visibility: Science and regulation. J. Air Waste Manag. 52, 973–999.

Wen, C.C., Yeh, H.H., 2010. Comparative influences of airborne pollutants and meteorological parameters on atmospheric visibility and turbidity. Atmos. Res. 96, 496–509.

Xu, J., Bergin, M.H., Yu, X., Zhao, J., Carrico, C.M., Baumann, K., 2002. Measurement of aerosol chemical, physical and radiative properties in the Yangtze delta region of China. Atmos. Environ. 36, 161–173.

Xue, D., Li, C.F., Liu, Q., 2015. Visibility characteristics and the impacts of air pollutants and meteorological conditions over Shanghai, China. Environ. Monit. Assess. 187, 363–373.

Yang, L.X., Wang, D.C., Chen, S.H., Wang, Z., Zhou, Y., Zhou, X.H., Wang, X.W., 2007. Influence of meteorological conditions and particulate matter on visual range impairment in Jinan, China. Sci. Total. Environ. 383, 164–173.

Yu, X.N., Ma, J., An, J.L., Yuan, L., Zhu, B., Liu, D.Y., Wang, J., Yang, Y., Cui, H.X., 2016. Impacts of meteorological condition and aerosol chemical compositions on visibility impairment in Nanjing, China. J. Clean. Prod. 131, 112–120.

Zhang, X.Y., Wang, Y.Q., Niu, T. Zhang, X.C., Gong, S.L., Zhang, Y.M., Sun, J.Y., 2012. Atmospheric aerosol compositions in China: spatial/temporal variability, chemical signature, regional haze distribution and comparisons with global aerosols. Atmos. Chem. Phys. 12, 779–799.

Zhang, Q.H., Zhang, J.P., Xue, H.W., 2010. The challenge of improving visibility in Beijing. Atmos. Chem. Phys. 10, 7821–7827.

Zhao, P.S., Zhang, X.L., Xu, X.F., Zhao, X.J., 2011. Long-term visibility trends and characteristics in the region of Beijing, Tianjin, and Hebei, China. Atmos. Res. 101, 711–718.

List of tables

Table 1 Regression models of visibility under different RH in DQL, June 2014-May 2015.

Stepwise regression model		correlation coefficient	N.
$V = 23.044+27.853*\exp(-0.04199PM_{2.5}) –0.196RH$	$RH \leq 80\%$	0.816	4247
$V = 56.072+24.44*\exp(-0.07128PM_{2.5}) –0.536RH-0.037O_3$	$80 < RH \leq 90\%$	0.671	2049
$V = 79.095+10.228*\exp(-0.06571PM_{2.5}) –0.822RH+0.033T$	$RH > 90\%$	0.589	1697

List of fugures

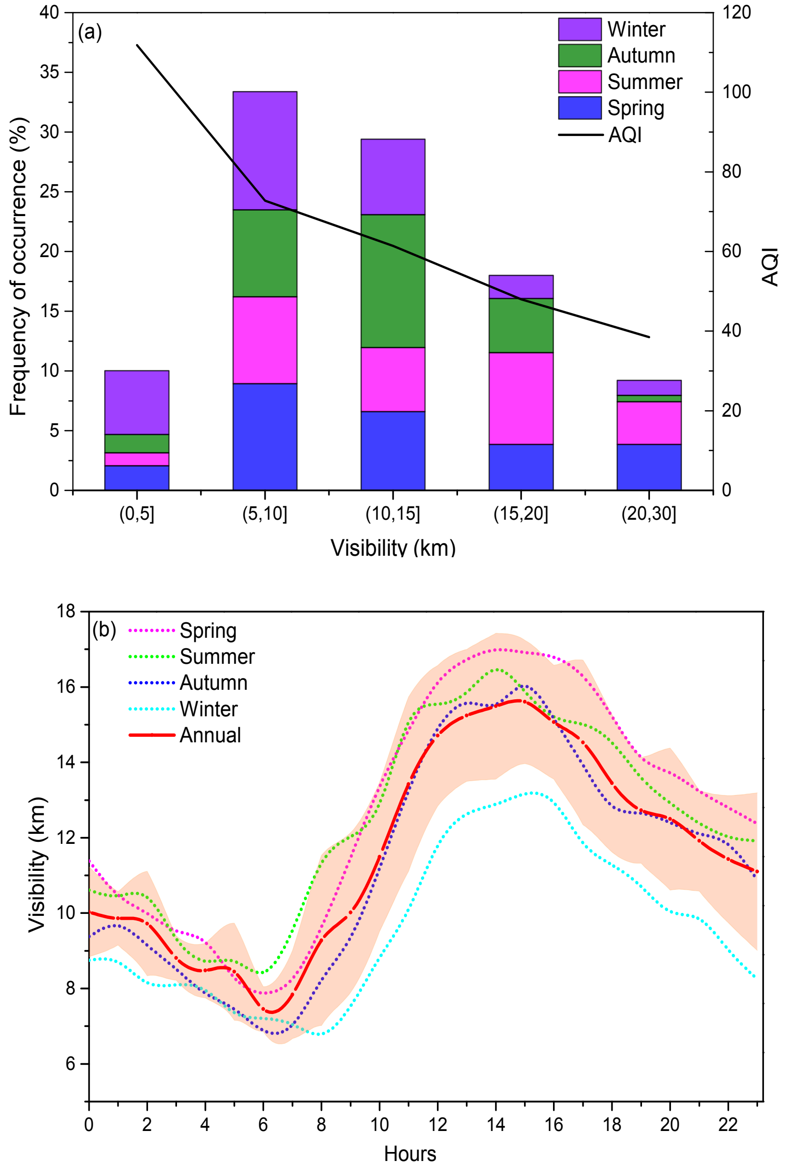

Fig. 1. Distribution of frequency of occurrence of daily visibility (a), and Diurnal variations of annual and seasonal visibility (b) at DQL in Ningbo. The shading area shows the standard deviations for the annual data.

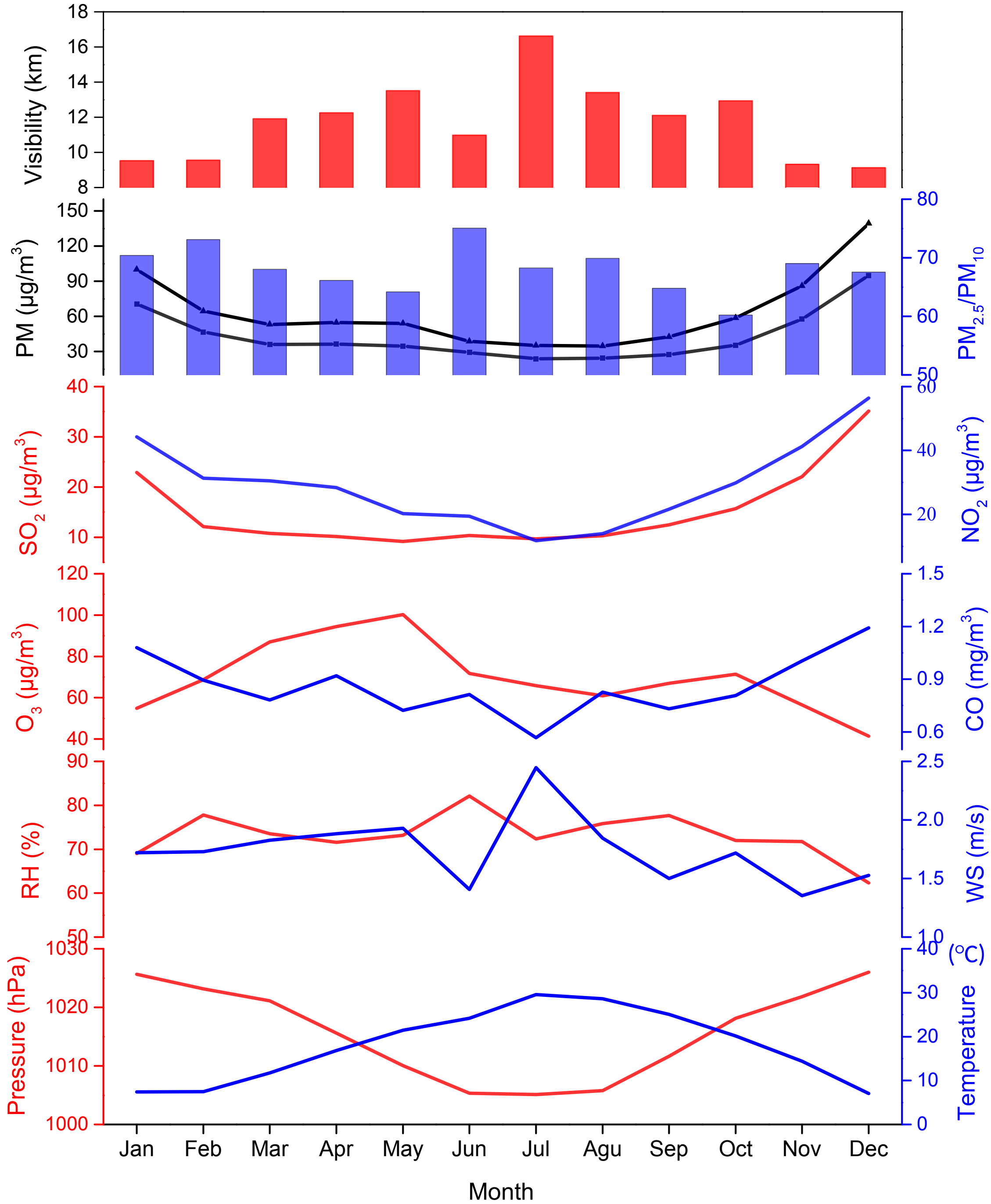

Fig. 2. Monthly variations of visibility and other environmental variables.

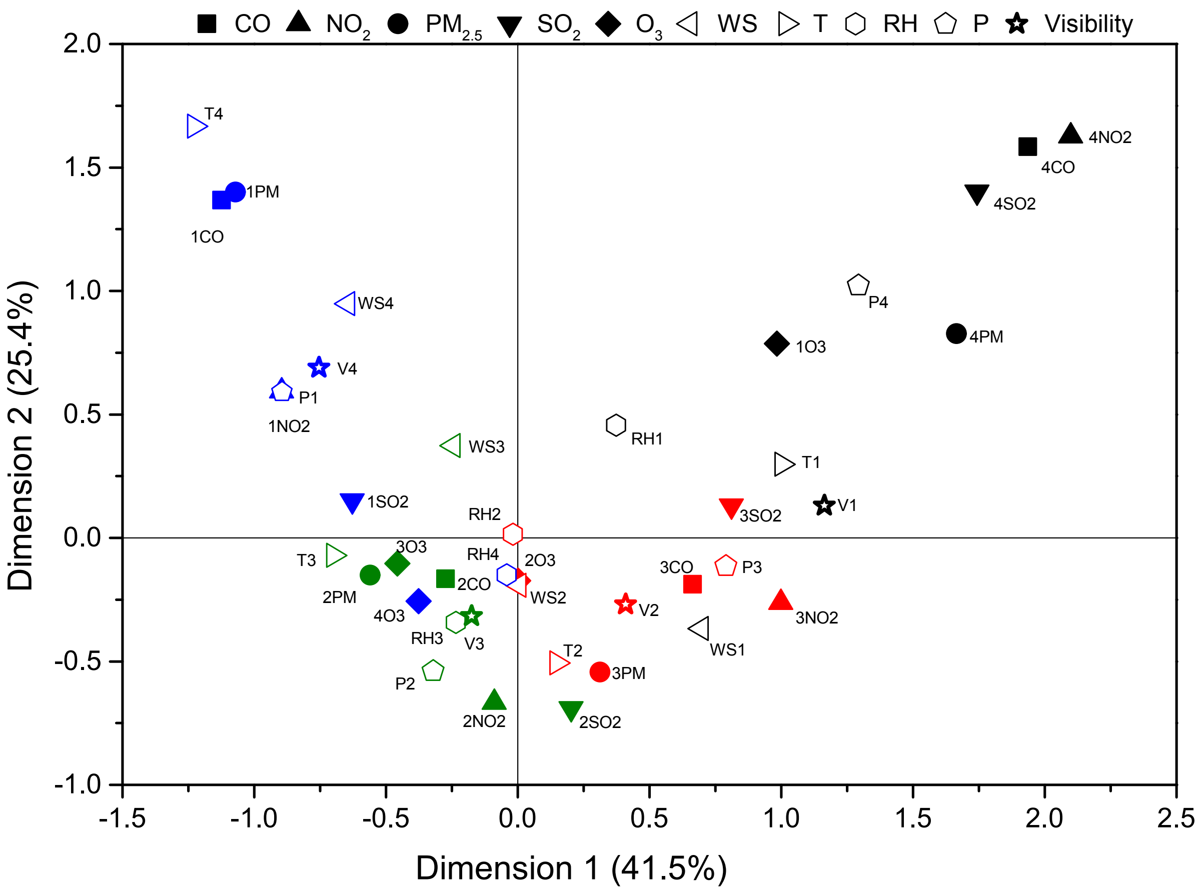

Fig. 3. Category quantification plot of classified visibility and other environmental variables at DQL.

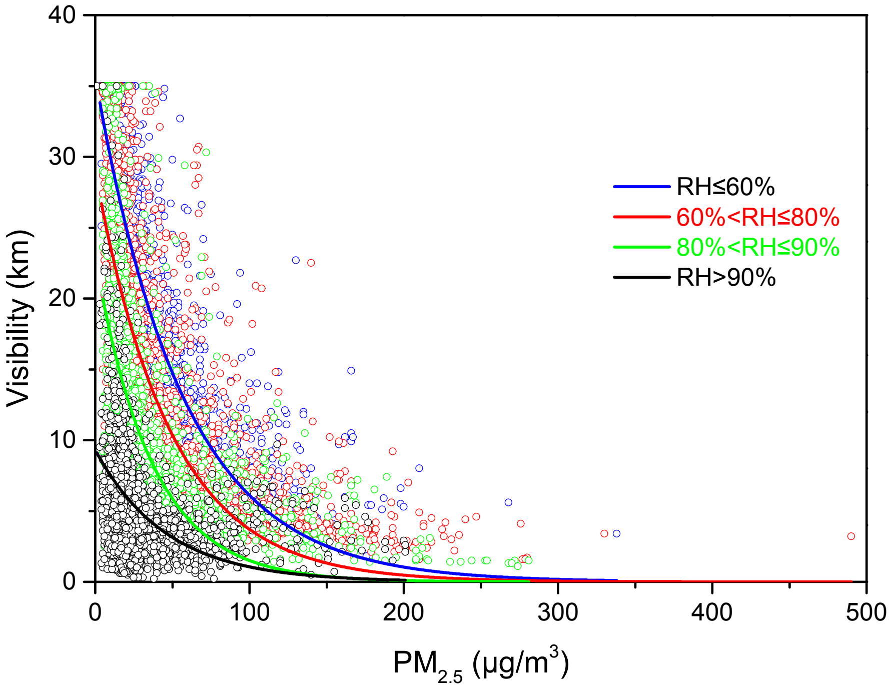

Fig. 4. Relationships between one-year visibility and $PM_{2.5}$ at DQL (2014.6.1–2015.5.31). Data points are color coded by RH. All the data are hourly average.

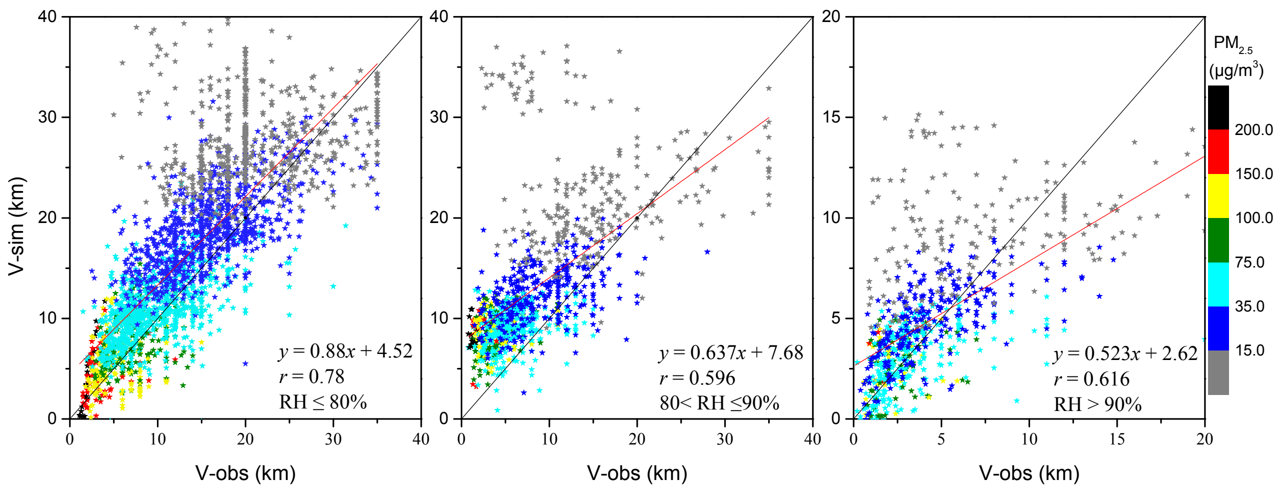

Fig. 5. Comparison between the observed hourly visibility and regression model simulated hourly visibility during 2013.6-2014.5. (V-obs: the observed visibility; V-sim: the simulated visibility).

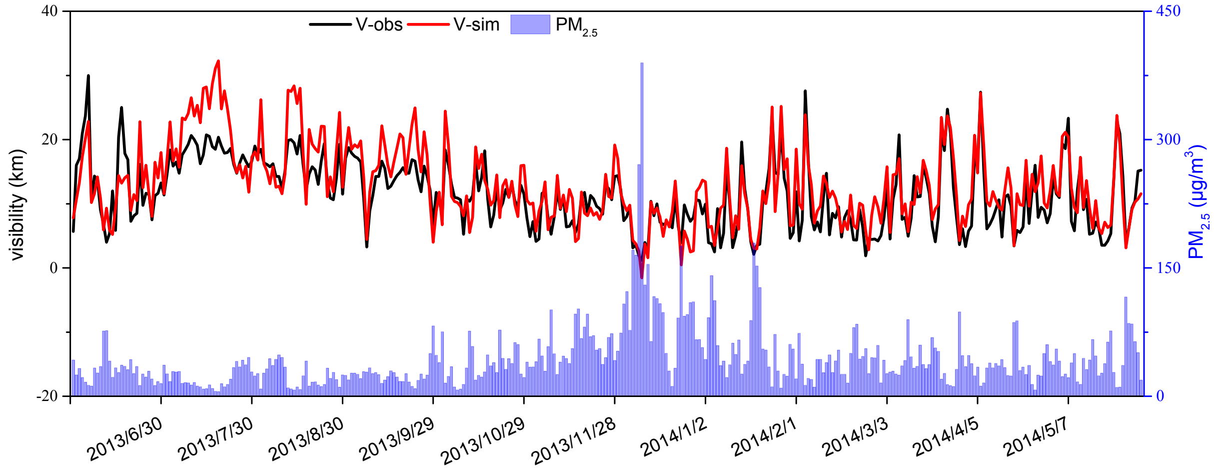

Fig. 6. Time series of daily observed visibility and daily simulated visibility by stepwise regression equations at DQL. (V-obs: the observed visibility; V-sim: the simulated visibility).

Supporting Materials

Temporal variability of visibility and its parameterizations in Ningbo, China

Jingjing Zhang[a, b, c, 1], Lei Tong[a, b, 1], Chenghui Peng[b, c], Huiling Zhang[a, c], Zhongwen Huang[a, c, d], Jun He[e], Hang Xiao[a, b, *]

[a] *Center for Excellence in Regional Atmospheric Environment, Institute of Urban Environment, Chinese Academy of Sciences, Xiamen 361021, China*

[b] *Key Lab of Urban Environment and Health, Institute of Urban Environment, Chinese Academy of Sciences, Xiamen 361021, China*

[c] *University of Chinese Academy of Sciences, Beijing 100049, China*

[d] *School of Chemistry and Environmental Engineering, Hanshan Normal University, Chaozhou, 521041, China*

[e] *International Doctoral Innovation Centre, Department of Chemical and Environmental Engineering, University of Nottingham Ningbo China, Ningbo, China*

*Corresponding author. Institute of Urban Environment, Chinese Academy of Sciences, Xiamen, China.

E-*mail address*: hxiao@iue.ac.cn

[1] The two authors contributed equally to this paper.

Table S1. Summary of visibility, AQI, and environmental factors from June, 2013 to May, 2015.

	Number	Min	Max	Mean	SD
Visibility (km)	730	0.6	34.1	11.8	5.9
AQI	717	12.7	428.9	65.6	39.0
$PM_{2.5}$ (μg/m^3)	717	5.3	389.8	42.6	33.4
PM_{10} (μg/m^3)	717	10.0	511.4	64.6	46.3
CO (mg/m^3)	717	0.1	2.6	0.9	0.3
NO_2 (μg/m^3)	717	0.5	98.3	28.9	17.6
SO_2 (μg/m^3)	717	2.0	76.2	15.0	12.3
O_3 (μg/m^3)	717	5.3	184.9	70.2	29.9
Temperature (°C)	730	0.5	34.2	17.8	8.4
Pressure (hPa)	730	996.2	1034.3	1013.0	8.7
RH (%)	730	31.8	96.6	73.2	12.5
WS (m/s)	730	0.1	4.8	1.7	0.8

Table S2. Indices of classified variables in MCA.

Categories	CO (mg/m^3)	NO_2 (μg/m^3)	$PM_{2.5}$ (μg/m^3)	SO_2 (μg/m^3)	P (Pa)	Color
1	0-0.5	0-20	0-15	0-10	990-1010	blue
2	0.5-1	20-40	15-35	10-20	1010-1020	green
3	1-1.5	40-60	35-75	20-40	1020-1030	red
4	>1.5	>60	>75	>40	1030-1040	black
Categories	**Vis (km)**	**RH (%)**	**WS (m/s)**	**T (℃)**	**O_3 (μg/m^3)**	**Color**
1	0<V<5	<60	0-1	0-10	0-40	black
2	5<V<10	60-80	1-2	10-20	40-80	red
3	10<V<15	80-90	2-3	20-30	80-120	green
4	V>15	>90	>3	30-40	>120	blue

Table S3. The discrimination measures of the variables in MCA.

	Dimension		
	1	2	Mean
CO	0.42	0.28	0.35
NO_2	0.77	0.47	0.62
$PM_{2.5}$	0.66	0.42	0.54
SO_2	0.54	0.30	0.42
O_3	0.14	0.18	0.16
WS	0.10	0.14	0.12
T	0.56	0.27	0.42
RH	0.06	0.05	0.06
P	0.59	0.24	0.41
V	0.31	0.18	0.25
Total	4.15	2.54	3.34
Variance (%)	41.5	25.4	33.4

Table S4. Pearson correlation coefficient of visibility and other environmental variables.

	Visibility	$PM_{2.5}$	CO	NO_2	SO_2	O_3	WS	RH	T	P
Visibility	1									
$PM_{2.5}$	–0.50**	1								
CO	–0.51**	0.68**	1							
NO_2	–0.47**	0.70**	0.54**	1						
SO_2	–0.18**	0.57**	0.40**	0.63**	1					
O_3	0.18**	–0.14**	–0.22**	–0.39**	–0.23**	1				
WS	0.39**	–0.26**	–0.19**	–0.27**	–0.14**	0.04	1			
RH	–0.40**	–0.22**	–0.07*	–0.15**	–0.40**	–0.23**	–0.20**	1		
T	0.30**	–0.45**	–0.37**	–0.65**	–0.40**	0.18**	0.15**	0.17**	1	
P	–0.18**	0.43**	0.33**	0.62**	0.43**	–0.18**	–0.19**	–0.29**	–0.89**	1
Rainfall	–0.13**	–0.17**	–0.08*	–0.13**	–0.07	–0.14**	–0.02	0.36**	0.11**	–0.17**

*Correlation is significant at the 0.05 level (two-tailed). ** Correlation is significant at the 0.01 level (two-tailed).

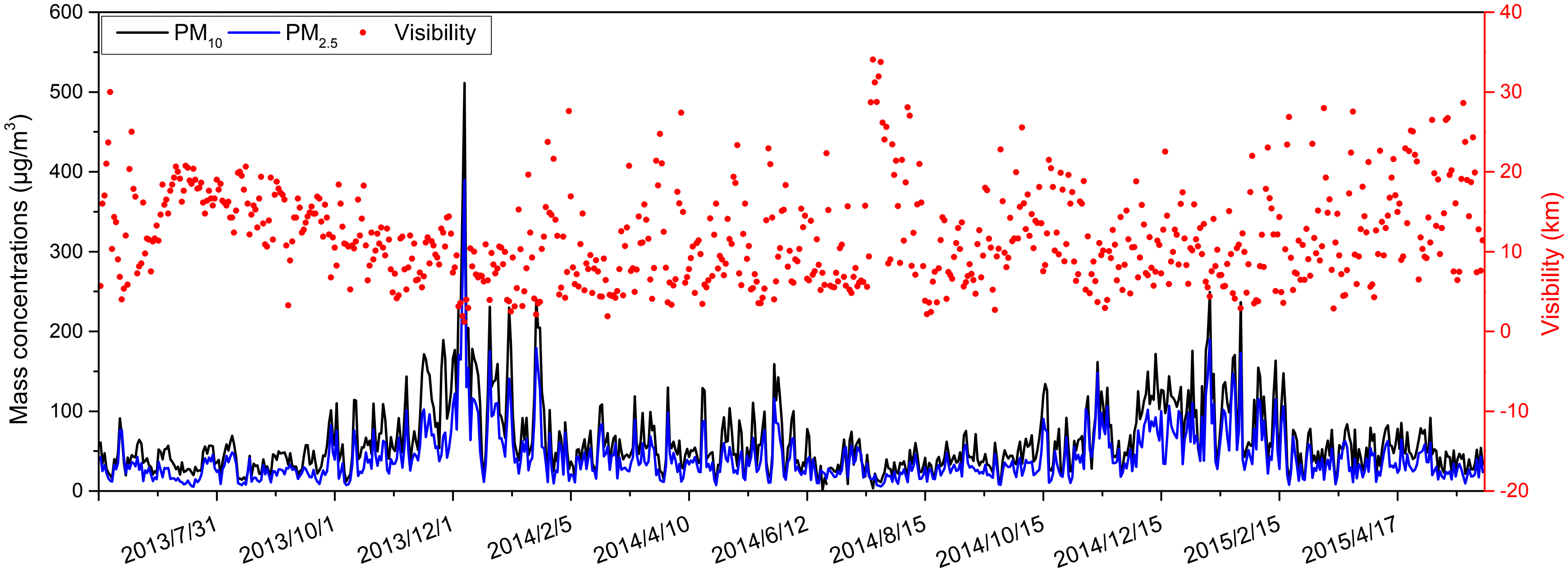

Fig. S1. Day-to-day variations of visibility, $PM_{2.5}$ and PM_{10} from June, 2013 to May, 2015 at DQL station in Ningbo.

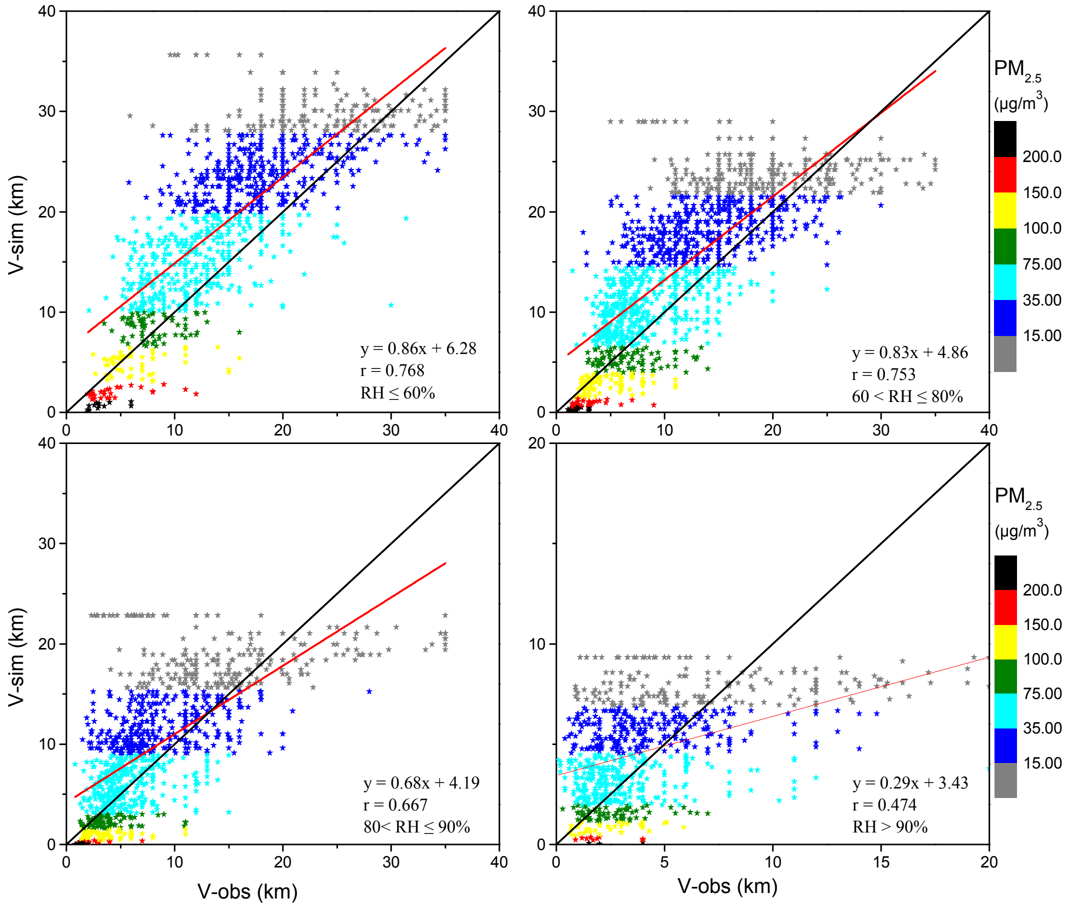

Fig. S2. Comparison between the observed hourly visibility and exponential equation (3) simulated hourly visibility during 2013.6-2014.5. (V-obs: the observed visibility; V-sim: the simulated visibility).

JOURNAL OF ENVIRONMENTAL SCIENCES

Editorial Department
P. O. Box 2871
Beijing 100085
China
Tel: 86-10-62920553
E-mail: jesc@rcees.ac.cn

Journal Publishing Agreement

Author(s): Jingjing Zhang, Lei Tong, Chonghui, Peng, Huiling. zhang, Zhongwan, Huang, Jun He, Hang xiao

Title:

Temporal variability of visibility and its parameterizations in Ningbo, China.

The undersigned authors, with the consent of all authors, hereby assign to *Journal of Environmental Sciences*, the copyright in the above identified article to be transferred, including supplemental tables, illustrations or other information submitted in all forms and media throughout the world, in all languages and format, effective when and if the article is accepted for publication.

Authors also agree to the following terms:

A. The article submitted is not subject to any prior claim or agreement and is not under consideration for publication elsewhere.
B. The article contains no libelous or other unlawful statements and does not contain any materials that violate proprietary right of any other person, company, organization, and nation.
C. If the article was prepared jointly with other authors, the author(s) agree with the authorship sequence.

Please sign and date the document.

First Author: 张晶晶,

Corresponding author:

Date: 2018.3.22

Date: 2018.3.22.